

# New precision mass measurements of neutron-rich calcium and potassium isotopes and three-nucleon forces

A.T. Gallant,<sup>1,2,\*</sup> J.C. Bale,<sup>1,3</sup> T. Brunner,<sup>1</sup> U. Chowdhury,<sup>1,4</sup> S. Ettenauer,<sup>1,2</sup> A. Lennarz,<sup>1,5</sup> D. Robertson,<sup>1</sup> V.V. Simon,<sup>1,6,7</sup> A. Chaudhuri,<sup>1</sup> J.D. Holt,<sup>8,9</sup> A.A. Kwiatkowski,<sup>1</sup> E. Mané,<sup>1</sup> J. Menéndez,<sup>10,11</sup> B.E. Schultz,<sup>1</sup> M.C. Simon,<sup>1</sup> C. Andreoiu,<sup>3</sup> P. Delheij,<sup>1</sup> M.R. Pearson,<sup>1</sup> H. Savajols,<sup>12</sup> A. Schwenk,<sup>11,10</sup> and J. Dilling<sup>1,2</sup>

<sup>1</sup>TRIUMF, 4004 Wesbrook Mall, Vancouver, British Columbia, V6T 2A3 Canada

<sup>2</sup>Department of Physics and Astronomy, University of British Columbia, Vancouver, British Columbia, V6T 1Z1 Canada

<sup>3</sup>Department of Chemistry, Simon Fraser University, Burnaby, BC V5A 1S6, Canada

<sup>4</sup>Department of Physics and Astronomy, University of Manitoba, Winnipeg, Manitoba, R3T 2N2 Canada

<sup>5</sup>Institut für Kernphysik Westfälische Wilhelms-Universität, 48149 Münster, Germany

<sup>6</sup>Fakultät für Physik und Astronomie, Ruprecht-Karls-Universität Heidelberg, 69120 Heidelberg, Germany

<sup>7</sup>Max-Planck-Institut für Kernphysik, 69117 Heidelberg, Germany

<sup>8</sup>Department of Physics and Astronomy, University of Tennessee, Knoxville, TN 37996, USA

<sup>9</sup>Physics Division, Oak Ridge National Laboratory, P.O. Box 2008, Oak Ridge, TN 37831, USA

<sup>10</sup>Institut für Kernphysik, Technische Universität Darmstadt, 64289 Darmstadt, Germany

<sup>11</sup>ExtreMe Matter Institute EMMI, GSI Helmholtzzentrum für Schwerionenforschung GmbH, 64291 Darmstadt, Germany

<sup>12</sup>GANIL, Boulevard Henri Becquerel, Boîte Postale 55027, F-14076 Caen Cedex 05, France

(Dated: April 11, 2012)

We present precision Penning-trap mass measurements of neutron-rich calcium and potassium isotopes in the vicinity of neutron number  $N = 32$ . Using the TITAN system the mass of  $^{51}\text{K}$  was measured for the first time, and the precision of the  $^{51,52}\text{Ca}$  mass values were improved significantly. The new mass values show a dramatic increase of the binding energy compared to those reported in the atomic mass evaluation. In particular,  $^{52}\text{Ca}$  is more bound by 1.74 MeV, and the behavior with neutron number deviates substantially from the tabulated values. An increased binding was predicted recently based on calculations that include three-nucleon (3N) forces. We present a comparison to improved calculations, which agree remarkably with the evolution of masses with neutron number, making neutron-rich calcium isotopes an exciting region to probe 3N forces at neutron-rich extremes.

The neutron-rich calcium isotopes present a key region for understanding shell structures and their evolution to the neutron dripline. This includes the standard doubly-magic  $^{48}\text{Ca}$  at  $N = 28$  and new shell closures at  $N = 32$  and possibly at  $N = 34$ . The calcium chain, with only valence neutrons, probes features of nuclear forces similar to the oxygen isotopes, which have been under intensive experimental and theoretical studies [1, 2]. While the oxygen isotopes have been explored even beyond the neutron dripline,  $^{52}\text{Ca}$  is the most neutron-rich nucleus where mass measurements and  $\gamma$ -ray spectroscopy have been done. Due to the extremely low production yields for  $N > 32$ , only the neutron-rich, mid-shell titanium and chromium isotopes have been reached to  $N = 34$ . This makes the semi-magic calcium chain in the vicinity of  $N = 32$  an important stepping stone towards the neutron dripline.

Phenomenological forces in the  $pf$  shell, such as the KB3G [3] and GXPF1 [4] interactions, have been fit to  $N \leq 32$  in the calcium isotopes, but they disagree markedly in their prediction for  $^{54}\text{Ca}$  and for a possible shell closure at  $N = 34$ . In addition, it is well known that calculations based only on two-nucleon (NN) forces do not reproduce  $^{48}\text{Ca}$  as a doubly-magic nucleus when neutrons are added to a  $^{40}\text{Ca}$  core [5]. Motivated by these deficiencies, the impact of 3N forces was recently investigated in the oxygen and calcium isotopes within the shell

model [2, 6, 7]. It was shown that chiral 3N forces provide repulsive contributions to valence neutron-neutron interactions. As neutrons are added, these are key for shell structure and spectroscopy, and for the determination of the neutron dripline. For calcium, the  $N = 28$  magic number was reproduced successfully, with a high  $2^+$  excitation energy, and in the vicinity of  $N = 32$ , the calculations based on NN and 3N forces generally predicted an increase in the binding energy compared to experimental masses [6].

Nuclear masses provide important information about the interplay of strong interactions within a nucleus and the resulting nuclear structure effects they elicit. The systematic study of masses has, for example, led to the discovery of the new magic number  $N = 16$  and has been key for understanding the island of inversion [8–10]. Currently, Penning traps [11] provide the most precise mass spectrometers for stable and unstable nuclei and are in use at almost all rare isotope beam facilities [12].

In this Letter, we present the first precision mass measurements of  $^{51,52}\text{Ca}$  and  $^{51}\text{K}$  performed at TRIUMF's Ion Trap for Atomic and Nuclear Science (TITAN) [13–15]. This presents the first direct mass measurements to  $N = 32$  in these nuclides, extending the measurements of a previous campaign [16]. For the calcium isotopes, we compare the evolution of the new TITAN mass values with neutron number to microscopic calculations based

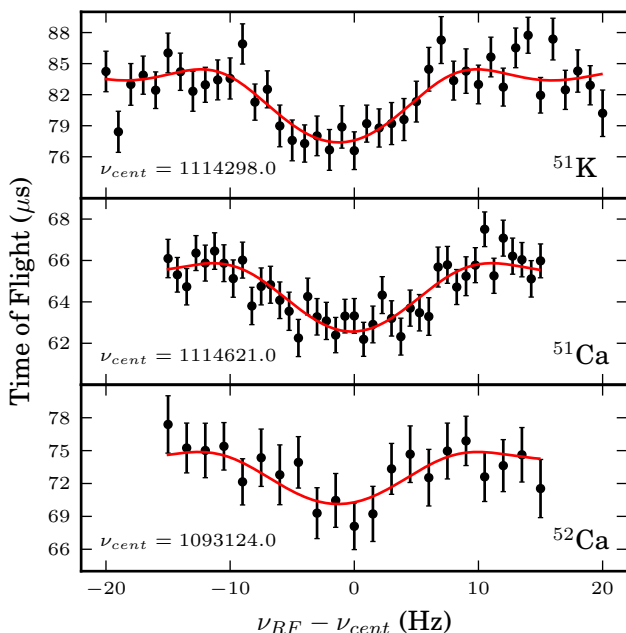


FIG. 1. (Color online) TOF-ICR resonances for  $^{51}\text{K}$ ,  $^{51}\text{Ca}$ , and  $^{52}\text{Ca}$  with excitation times of  $\approx 80$  ms. The applied radio-frequency  $\nu_{RF}$  is given as the difference from the center frequency  $\nu_{cent}$  of the scan range. The solid lines are theoretical fits to the line shape [18].

on chiral NN and 3N forces.

The  $^{51,52}\text{Ca}$  isotopes were produced at TRIUMF's Isotope Separator and Accelerator (ISAC) facility by bombarding a high-power tantalum target with a  $70 \mu\text{A}$  proton beam of 480 MeV energy, and a resonant laser ionization scheme [17] was used to enhance the ionization of the beam.  $^{51}\text{K}$  was produced with  $1.9 \mu\text{A}$  of protons on a  $\text{UC}_x$  target, and ionized using a surface source. The continuous ion beam was extracted from the target, mass separated with the ISAC dipole separator system, and delivered to the TITAN facility. TITAN uses the time-of-flight ion cyclotron-resonance (TOF-ICR) [18] method on singly-charged [19–21] and highly-charged [22] ions for precision mass measurements and is capable of accurate measurements in the parts-per-billion (ppb) precision range [23]. The system consists of a helium-buffer-gas-filled radio-frequency quadrupole [24] for cooling and bunching, followed by, in this case bypassed, an electron beam ion trap charge breeder (EBIT) [25], and a precision Penning trap [15], where the mass was determined.

In the precision Penning trap a homogenous 3.7 T magnetic field radially confines the injected ions, while an electric quadrupole field provides axial confinement. In order to determine an ion's mass  $m$ , the cyclotron frequency  $\nu_c = qB/(2\pi m)$ , where  $q$  is the charge of the ion and  $B$  is a homogeneous magnetic field, is determined from the minimum of the TOF-ICR measurement. Typ-

ical TOF-ICR resonances for  $^{51}\text{K}$ ,  $^{51}\text{Ca}$ , and  $^{52}\text{Ca}$  are shown in Fig. 1. To calibrate the magnetic field, measurements with a reference ion of well-known mass were taken before and after the frequency measurement of the ion of interest. To eliminate magnetic field fluctuations a linear interpolation of the reference frequency to the center time of the measurement of  $\nu_c$  is performed, and a ratio of the frequencies  $R = \nu_{c,ref}/\nu_c$  is taken. The atomic mass  $m_a$  of interest can then be extracted from the average frequency ratio  $\bar{R}$ ,  $m_a = \bar{R}(m_{a,ref} - m_e) + m_e$  where  $m_e$  is the mass of the electron.

To reduce systematic effects, such as those arising from field misalignments, incomplete trap compensation, etc., a reference with a similar mass was chosen [15]. For the measurements where a mass doublet was not formed a mass measurement of  $^{41}\text{K}$  relative to  $^{58}\text{Ni}$  was performed to investigate the mass-dependent shift. The mass of  $^{41}\text{K}$  was in agreement with Ref. [26], constraining the mass-dependent shift to be below 3.5 ppb in the frequency ratio. We include this shift as a systematic uncertainty. Moreover, to exclude potential effects stemming from ion-ion interactions from simultaneously stored isobars, contaminants were eliminated from the trap by applying a dipolar field at the mass-dependent reduced cyclotron frequency  $\nu_+$  for 20 ms prior to the quadrupole excitation. Dipole cleaning pushes the contaminants far from the precision confinement volume, greatly reducing any potential shifts due to their Coulomb interaction with the ion of interest. A quadrupole excitation time of  $\approx 80$  ms was used for each of the mass measurements. In addition, a count class analysis [27] was performed when the count rate was high enough to permit such an analysis. In cases where the rate was too low, the frequency ratio was determined twice: Once where only one ion was detected, and a second time where all detected ions were included. The ion-ion interaction systematic uncertainty was taken to be the difference between these two methods and was 100 ppb for  $^{51}\text{K}$  and 750 ppb for  $^{52}\text{Ca}$ .

In previous works, mass measurements for neutron-rich potassium and calcium isotopes were reported up to  $^{50}\text{K}$  and  $^{52}\text{Ca}$  [28, 29], but with large uncertainties. While the half-lives in the vicinity of  $N = 32$  are generally long ( $t_{1/2} > 50$  ms), the production yields in this high  $N/Z$  region have limited precision mass measurements until now. The mass of  $^{51}\text{Ca}$ , as tabulated in the atomic mass evaluation (AME2003) [29], depends largely on three-neutron-transfer reactions from beams of  $^{14}\text{C}$  or  $^{18}\text{O}$  to a  $^{48}\text{Ca}$  target [30–33]. Measurements by different groups using the same reaction lead to differing results, calling into question the derived mass. Further problems with the reaction methods include potential  $^{40}\text{Ca}$  contamination in the target, disagreement on the number and excitation energies of observed states, and low statistics. In addition, two TOF measurements of the  $^{51}\text{Ca}$  mass [28, 34] are in agreement with each other, but disagree with the values derived from the three-neutron-

TABLE I. Measured average frequency ratios  $\bar{R}$  and mass excess (ME) with total error of  $^{51,52}\text{Ca}$  and  $^{51}\text{K}$ , compared to the AME2003 mass excess. The \* indicates that the AME2003 value for  $^{51}\text{K}$  is based on an extrapolation.

Isotope	Reference	$R = \nu_{c,ref}/\nu_c$	ME (keV)	ME <sub>AME03</sub> (keV)	ME-ME <sub>AME03</sub> (keV)
$^{51}\text{Ca}$	$^{58}\text{Ni}$	0.87961718(42)	-36338.9(22.7)	-35863.3(93.8)	-475.6(96.5)
$^{52}\text{Ca}$	$^{58}\text{Ni}$	0.89691649(187)	-34260.0(101.0)	-32509.1(698.6)	-1751.0
$^{52}\text{Ca}$	$^{52}\text{Cr}$	1.00043782(158)	-34235.8(76.4)	same	-1726.7
$^{52}\text{Ca}$ Average:			-34244.6(61.0)	same	-1735.5(701.3)
$^{51}\text{K}$	$^{51}\text{V}$	1.00062561(28)	-22516.3(13.1)	-22002.0(503.0)*	-514.3(503.2)

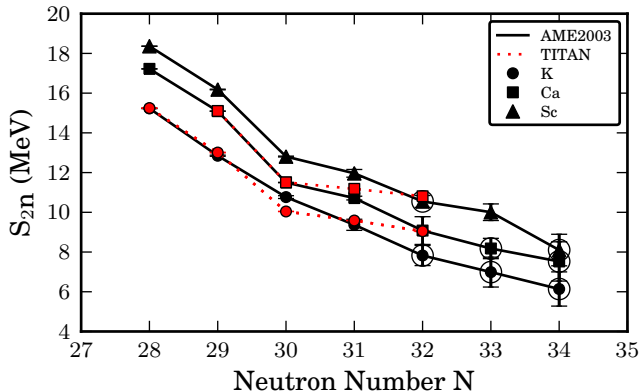


FIG. 2. (Color online) Two-neutron separation energy  $S_{2n}$  as a function of neutron number  $N$  for the potassium (circles), calcium (square), and scandium (triangles) isotopic chains. Points enclosed by a circle are not based completely on experimental values in AME2003. The symbols connected by a dotted line are based on the TITAN mass values (mass values for  $^{49,50}\text{Ca}$  and  $^{47-50}\text{K}$  are taken from Ref. [16]), while the symbols connected by solid lines are those from the AME2003.

transfer reactions. However, the uncertainties reported are 2–10 times larger than those obtained from the reactions. All masses tabulated in the AME2003 disagree with the presented measurement by more than  $1\sigma$ . More recently, a TOF mass measurement was completed at the GSI storage ring [35]. This does not agree with any of the previous measurements and deviates by  $1.3\sigma$  from the value presented in this Letter. For  $^{52}\text{Ca}$ , the existing mass value is derived from a TOF measurement [28] and a  $\beta$ -decay measurement to  $^{52}\text{Sc}$  [36]. Neither measurement agrees with our precision mass. No experimental data exists for the mass of  $^{51}\text{K}$ .

Our new TITAN mass measurements for  $^{51,52}\text{Ca}$  and  $^{51}\text{K}$  are presented in Table I. The mass of  $^{51}\text{Ca}$  deviates by  $5\sigma$  from the AME2003 and is more bound by 0.5 MeV. We find a similar increase in binding for  $^{51}\text{K}$  compared to the AME2003 extrapolation. For the most neutron-rich  $^{52}\text{Ca}$  isotope measured, the mass is more bound by 1.74 MeV compared to the present mass table. This dramatic increase in binding leads to a pronounced change of the derived two-neutron separation energy  $S_{2n}$  in the vicinity of  $N = 32$ , as shown in Fig. 2. The re-

sulting behavior of  $S_{2n}$  in the potassium and calcium isotopic chains with increasing neutron number is significantly flatter from  $N = 30$  to  $N = 32$ . This also differs from the scandium isotopes, derived from previously measured mass excess with large uncertainties or from the AME2003 extrapolation. The increased binding for the potassium and calcium isotopes may indicate the development of a significant subshell gap at  $N = 32$ , in line with the observed high  $2^+$  excitation energy in  $^{52}\text{Ca}$ [36].

Three-nucleon forces have been unambiguously established in light nuclei, but only recently explored in medium-mass nuclei [2, 6, 7, 37, 38]. These advances have been driven by chiral effective field theory, which provides a systematic expansion for NN, 3N and higher-body forces [39], combined with renormalization group methods to evolve nuclear forces to lower resolution [40].

We follow Ref. [6] and calculate the two-body interactions among valence neutrons in the extended  $pf g_{9/2}$  shell on top of a  $^{40}\text{Ca}$  core, taking into account valence-core interactions in 13 major shells based on a chiral  $\text{N}^3\text{LO}$  NN potential evolved to low-momentum. Chiral 3N forces are included at  $\text{N}^2\text{LO}$ , where the two shorter-range 3N couplings have been fit to the  $^3\text{H}$  binding energy and the  $^4\text{He}$  charge radius. For valence neutrons the dominant contribution is due to the long-range two-pion-exchange part of 3N forces [2, 6]. In Ref. [6], the normal-ordered one- and two-body parts of 3N forces were included to first order, and an increased binding in the vicinity of  $N = 32$  was predicted. Here, we improve the calculation by including the one- and two-body parts of 3N forces in 5 major shells to third order, on an equal footing as NN interactions. This takes into account the effect of 3N forces between nucleons occupying orbits above and below the valence space. For the single-particle energies (SPEs) in  $^{41}\text{Ca}$ , we study two cases: The SPEs obtained by solving the Dyson equation, where the self-energy is calculated consistently in many-body perturbation theory (MBPT) to third order; and empirical (emp) SPEs where the  $pf$ -orbit energies are taken from Ref. [4] and the  $g_{9/2}$  energy is set to  $-1.0$  MeV.

In Fig. 3 we compare the theoretical results obtained from exact diagonalizations in the valence space to the TITAN and AME2003 values for the two-neutron separation energy and for the neutron pairing gap calculated from three-point binding-energy differences,  $\Delta_n^{(3)} =$

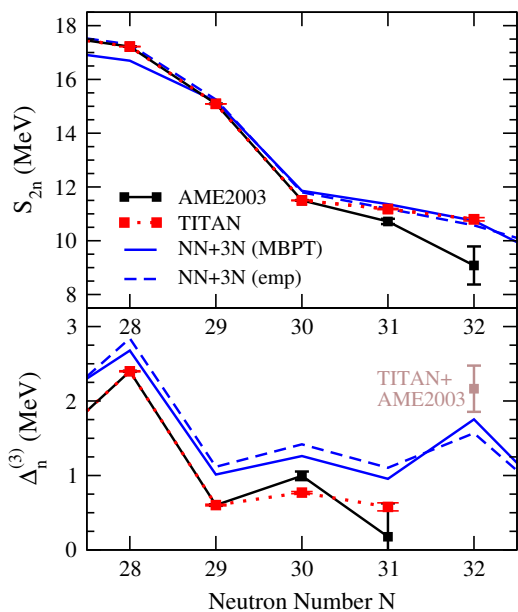


FIG. 3. (Color online) Two-neutron separation energy  $S_{2n}$  (top) and pairing gap  $\Delta_n^{(3)}$  from three-point binding-energy differences (bottom) versus neutron number  $N$  for the calcium isotopes. The TITAN mass values and the AME2003 values are shown by the symbols as in Fig. 2. The point labelled “TITAN+AME2003” is based partly on the TITAN mass values and complemented by the AME2003 value for  $^{53}\text{Ca}$ . Theoretical predictions are shown based on chiral NN and 3N forces (NN+3N) in the extended  $pf_{g_{9/2}}$  valence space using empirical (emp) SPEs in  $^{41}\text{Ca}$  and consistently calculated MBPT SPEs (MBPT).

$(-1)^N [B(N+1, Z) + B(N-1, Z) - 2B(N, Z)]/2$ . The predicted  $S_{2n}$  is very similar for both sets of SPEs and is in excellent agreement with the new TITAN mass values. For  $^{51,52}\text{Ca}$ , the difference between theory and experiment is only  $\lesssim 200$  keV, but we emphasize that it will be important to also study the impact of the uncertainties in the leading 3N forces. The behavior with neutron number for  $\Delta_n^{(3)}$  is also well reproduced, but the theoretical gaps are typically 500 keV larger. Finally, we note also the developments using nonempirical pairing functionals in this region [41], which provide a bridge to global energy-density functional calculations.

In summary, the mass of  $^{51}\text{K}$  has been measured with the TITAN facility at TRIUMF for the first time, and the new precision masses of  $^{51,52}\text{Ca}$  show a dramatic increase in binding compared to the atomic mass evaluation. The most neutron-rich  $^{52}\text{Ca}$  is more bound by 1.74 MeV, a value similar in magnitude to the deuteron binding energy. An increased binding around  $N = 32$  was predicted recently in calculations based on chiral NN and 3N forces [6]. The new TITAN results lead to a substantial change in the evolution of nuclear masses to neutron-rich extremes. The significantly flatter behavior

of the two-neutron separation energy agrees remarkably well with improved theoretical calculations including 3N forces, making neutron-rich calcium isotopes an exciting region to probe 3N forces and to test their predictions towards the neutron dripline. These developments are of great interest also for astrophysics, as similar changes in heavier nuclei would have a dramatic impact on nucleosynthesis [42], and the same 3N forces provide important repulsive contributions in neutron-star matter [43].

This work was supported by NSERC and the NRC Canada, the US DOE Grant DE-FC02-07ER41457 (UN-EDF SciDAC Collaboration) and DE-FG02-96ER40963 (UT), the Helmholtz Alliance HA216/EMMI, and the DFG through Grant SFB 634. Part of the numerical calculations have been performed on Kraken at the NICS. A.T.G. acknowledges support from the NSERC CGS-D program, S.E. from the Vanier CGS program, T.B. from the Evangelisches Studienwerk e.V. Villigst, V.V.S from the Studienstiftung des Deutschen Volkes, and A.L. from the DFG under Grant FR601/3-1.

\* Corresponding author: agallant@triumf.ca

- [1] T. Baumann, A. Spyrou, and M. Thoennessen, Rep. Prog. Phys. **75**, 036301 (2012).
- [2] T. Otsuka *et al.*, Phys. Rev. Lett. **105**, 032501 (2010).
- [3] A. Poves *et al.*, Nucl. Phys. A **694**, 157 (2001).
- [4] M. Honma *et al.*, Phys. Rev. C **65**, 061301(R) (2002).
- [5] E. Courrier *et al.*, Rev. Mod. Phys. **77**, 427 (2005).
- [6] J. D. Holt *et al.*, arXiv:1009.5984 (2010).
- [7] J. D. Holt *et al.*, arXiv:1108.2680 (2011).
- [8] C. Thibault *et al.*, Phys. Rev. C **12**, 644 (1975).
- [9] F. Sarazin *et al.*, Phys. Rev. Lett. **84**, 5062 (2000).
- [10] B. Jurado *et al.*, Phys. Lett. B **649**, 43 (2007).
- [11] K. Blaum, Phys. Rep. **425**, 1 (2006).
- [12] H.-J. Kluge, Hyperfine Interact. **196**, 295 (2010).
- [13] J. Dilling *et al.*, Nucl. Instrum. Methods Phys. Res. Sect. B **204**, 492 (2003).
- [14] J. Dilling *et al.*, Int. J. Mass Spectrom. **251**, 198 (2006).
- [15] M. Brodeur *et al.*, Int. J. Mass Spectrom. **310**, 20 (2012).
- [16] A. Lapierre *et al.*, Phys. Rev. C **85**, 024317 (2012).
- [17] J. Lassen *et al.*, in *Laser 2004*, edited by Z. Baszczyk, B. Markov, and K. Marinova (Springer, 2006) pp. 69–75.
- [18] M. König *et al.*, Int. J. Mass Spectrom. **142**, 95 (1995).
- [19] M. Smith *et al.*, Phys. Rev. Lett. **101**, 202501 (2008).
- [20] M. Brodeur *et al.*, Phys. Rev. Lett. **108**, 052504 (2012).
- [21] R. Ringle *et al.*, Phys. Lett. B **675**, 170 (2009).
- [22] S. Ettenauer *et al.*, Phys. Rev. Lett. **107**, 212501 (2011).
- [23] M. Brodeur *et al.*, Phys. Rev. C **80**, 044318 (2009).
- [24] T. Brunner *et al.*, Nucl. Instrum. Methods Phys. Res. Sect. A **676**, 32 (2012).
- [25] A. Lapierre *et al.*, Nucl. Instrum. Methods Phys. Res. Sect. A **624**, 54 (2012).
- [26] B. J. Mount, M. Redshaw, and E. G. Myers, Phys. Rev. A **82**, 042513 (2010).
- [27] A. Kellerbauer *et al.*, Eur. Phys. J. D **22**, 53 (2003).
- [28] X. L. Tu *et al.*, Z. Phys. A: At. Nucl. **337**, 361 (1990).
- [29] G. Audi, A. H. Wapstra, and C. Thibault, Nucl. Phys.

- A **729**, 337 (2003).
- [30] W. Mayer *et al.*, Phys. Rev. C **22**, 2449 (1980).
  - [31] W. Benenson *et al.*, Phys. Lett. B **162**, 87 (1985).
  - [32] M. Brauner *et al.*, Phys. Lett. B **150**, 75 (1985).
  - [33] W. N. Catford *et al.*, Nucl. Phys. A **489**, 347 (1988).
  - [34] H. L. Seifert *et al.*, Z. Phys. A: At. Nucl. **349**, 25 (1994).
  - [35] M. Matoš, Ph.D. thesis, Justus-Liebig-Universität Giessen (2004).
  - [36] A. Huck *et al.*, Phys. Rev. C **31**, 2226 (1985).
  - [37] R. Roth *et al.*, arXiv:1112.0287 (2011).
  - [38] G. Hagen *et al.*, arXiv:1202.2839 (2012).
  - [39] E. Epelbaum, H.-W. Hammer, and U.-G. Meißner, Rev. Mod. Phys. **81**, 1773 (2009).
  - [40] S. K. Bogner, R. J. Furnstahl, and A. Schwenk, Prog. Part. Nucl. Phys. **65**, 94 (2010).
  - [41] T. Lesinski *et al.*, J. Phys. G **39**, 015108 (2012).
  - [42] A. Arcones and G. F. Bertsch, arXiv:1111.4923 (2011).
  - [43] K. Hebeler *et al.*, Phys. Rev. Lett. **105**, 161102 (2010).